İSTANBUL UNIVERSITY CERRAHPAŞA

ORIGINAL ARTICLE
Electrica 2024; 24(3): 660-669

Proposal of an Optimal Control of an Electric Vehicle by Combined FOC and DTC Techniques

Saad Taa, Bachir Mokhtari

LEDMASD Laboratory, Department of Electrotechnics, Faculty of Technology, University of Laghouat, Algeria

Cite this article as: S. Taa and B. Mokhtari, "Proposal of an optimal control of an electric vehicle by combined FOC and DTC techniques," *Electrica*, 24(3), 660-669, 2024.

ABSTRACT

This work is the continuation of a research project launched 4 years ago, concerning the optimization of the propulsion of an electric vehicle, which is divided into two major axes: one deals with the signal processing part used for dynamics and the other deals with control techniques for vehicle driving. In this paper, we present our idea for the optimization of propulsion. We propose to use a combined control of field-oriented control (FOC) and direct torque control (DTC). The two well-known techniques have different advantages depending on whether you are looking at speed or torque. The vehicle is driven by a permanent magnet synchronous motor (PMSM). Throughout the journey, we apply a FOC to control the speed where the road is flat, and we apply a DTC whenever we need the desired torque. Switching between the two control techniques is ensured by a well-adjusted switch via the variation of the load torque obtained by the vehicle dynamics sensors. The results obtained show good stability of the proposed system and allow the intended operation of the propulsion system.

***Index Terms*—**Direct torque control, field oriented control, permanent magnet synchronous motor, position sensor, switcher

I. INTRODUCTION

In [1], we said that our work aims to implement a combination of the two control techniques, fieldoriented control (FOC) and direct torque control (DTC). We have therefore published the part that concerns the vehicle motion sensing system, and in this present work, we will present the second part of this great project.

The movement of the vehicle is based on two main parameters: one is the torque exerted on its driving wheels and the other is the speed. The two parameters mentioned are controlled through the FOC when the trajectory is on a flat road and the DTC if the road is on a slope.

We choose the permanent magnet synchronous motor (PMSM), which has received increasing acceptance in industrial applications due to its features of high efficiency, low noise, high performance, and robustness. It plays a fundamental role in manufacturing automation, such as in robotics, electric scooters, hybrid vehicles, elevators, aerospace, and applications in aircraft [2-6].

Direct torque control is characterized by its simplicity and very good dynamic response in torque, as well as the possibility of carrying out torque control without resorting to the speed or position loop [5, 7-9].

Field-oriented control is widely used in controlling PMSM drives to achieve fast four-quadrant operation, good acceleration, and smooth starting, and in this control process, the precise rotor position is needed. Usually, the rotor position and speed can be measured by an encoder or other kinds of sensors. However, the presence of these sensors causes problems such as cost, reliability, and installation complexity [10, 11].

In order to remedy these problems, research has been directed toward sensorless vector control for these motors in recent years [10]; therefore, vector control methods with oriented rotor flux in the absence of any position or speed sensor have been studied by many researchers in the scientific literature. Other techniques proposed in the literature are generally based on extended Kalman filters, state observers or *Luenberger* observers, and the model reference adaptive system (MRAS) method

Corresponding author:
Bachir Mokhtari

E-mail:
ba.mokhtari@lagh-univ.dz

Received: August 15, 2023

Revision Requested: August 22, 2023

Last Revision Received: July 25, 2024

Accepted: August 22, 2024

Publication Date: October 8, 2024

DOI: 10.5152/electrica.2024.23125

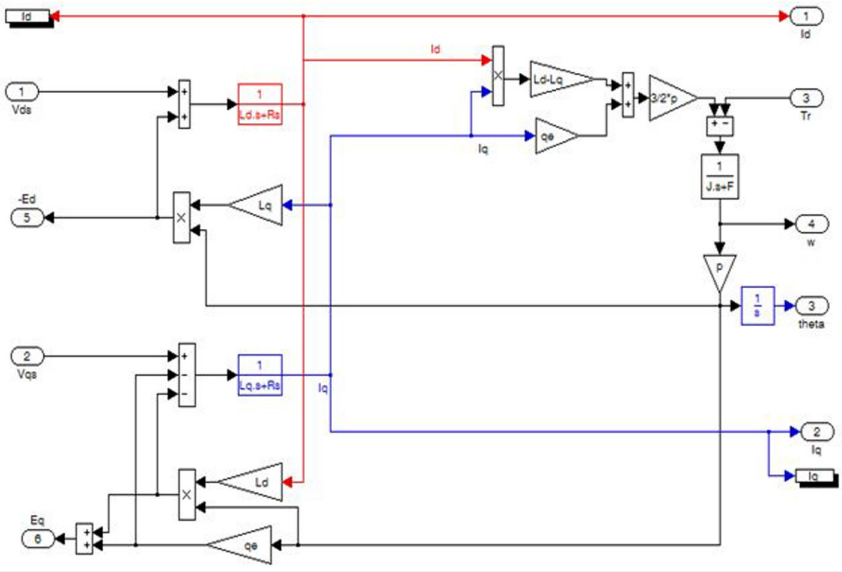

Fig. 1. The used permanent magnet synchronous motor model.

[12-17]. Comparison techniques between DTC control and other techniques applied in electric vehicles are presented by several researchers to determine the best choice of propulsion system [18]. The DTC is considered as a better strategy used in EVs; for this reason, researchers are always trying to improve it by reducing the ripples encountered in electromagnetic torque and stator magnetic flux [19-21].

Our contribution is to implement advanced control techniques to provide adequate propulsion for different roads. The combination of FOC and DTC ensures good road holding for the vehicle regardless of the nature of the road (flat or on a slope). In [1], we tested the performance of vehicle dynamics sensing systems formed from different proposed sensors. In this article, we will use them to provide information on the switching instant between the two control techniques.

This study is devoted to the modeling of the PMSM studied and the presentation of two control techniques. We then present the hybridization proposed to equip the electric vehicle. Finally, the results will be presented and discussed.

II. MODEL OF PERMANENT MAGNET SYNCHRONOUS MOTOR

To represent the motor in a model appropriate to the two used controls, we adopt a representation of the same system in a frame ($\alpha\beta$) linked to the stator.

This does not pose any problem because these representations are in an equivalent virtual space that only develops the signals which infuse the physical behavior of the real system.

However, it should be noted that for optimization of energy resources, we have opted to deactivate the control unit which does not work during the movement of the vehicle. In this paper, we prefer to represent the model via a diagram to facilitate its implementation under Simulink/Matlab. For more details of the model under mathematical formulas, one can consult [17, 22]. The model of the PMSM that we retained in this study is represented by Fig. 1.

III. Description of the Hybrid Propulsion Proposed

The FOC, as well as its associate the DTC, are well known in the literature of electrical controls [23, 24]. In this paper, we avoid citing them in detail and just recall the essentials.

A. FieldOriented Control

The FOC consists of controlling the stator currents. It is based on the transformation of the system of three-phase currents depending on time and speed into a time-invariant system with two coordinates *d* and *q*. These projections lead to a structure similar to that of a DC motor [11, 25].

The FOC needs two input references: the torque component (collinear with the q coordinate) and the flux component (collinear with the d coordinate). This control is more precise in transient and steady states [24].

The basic principle of PMSM control is based on the orientation of the rotor flux. Since the magnetic flux generated by the rotor of the PMSM is fixed relative to the position of the rotor shaft, it can be determined by the shaft position sensor [24].

If $I_{sd}=0$, the *d*-axis flux linkage φ_{sd} takes a constant value. Since φ_f is constant for a PMSM, this implies the proportionality of the electromagnetic torque to I_{sq} which is determined by closed-loop control [11, 24] and can be written by the following expression:

$$T_{em}=\frac{3}{2}pI_{sq}\varphi_f \tag{1}$$

1) Stator voltage Decoupling

The stator voltage equations are decoupled as follows [26]:

$$\begin{cases} V_{sd}=V_{sdref}+e_{sq} \\ V_{sq}=V_{sqref}+e_{sd} \end{cases} \tag{2}$$

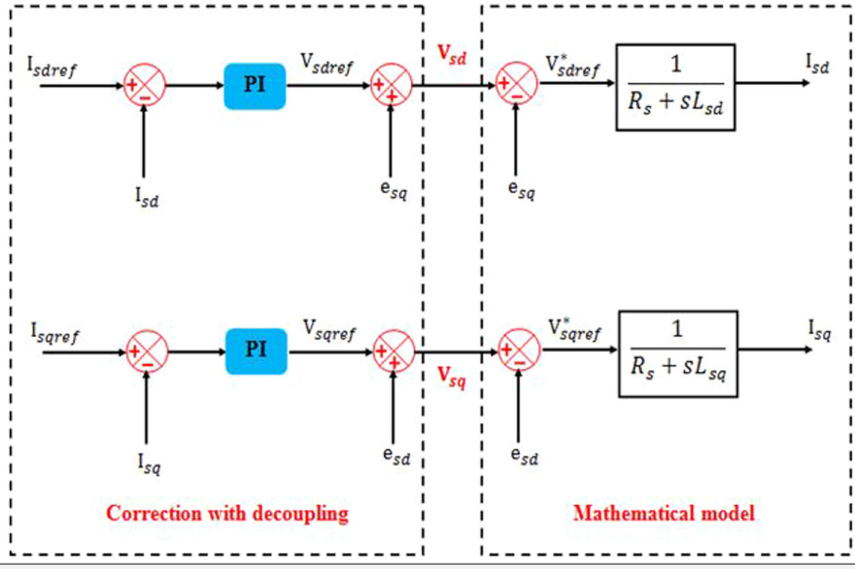

Fig. 2. Decoupling system principle.

Where:

$$\begin{cases} e_{sq} = -\omega L_q I_{sq} \\ e_{sd} = \omega L_d I_{sd} + \omega \varphi_f \end{cases} \quad (3)$$

The decoupling system is shown in Figure 2.

2) SPEED AND CURRENT CONTROL

The control block diagram for the current loop after decoupling and the speed loop can be generally derived. The current loop of a PMSM can be simplified as shown in Fig. 3.

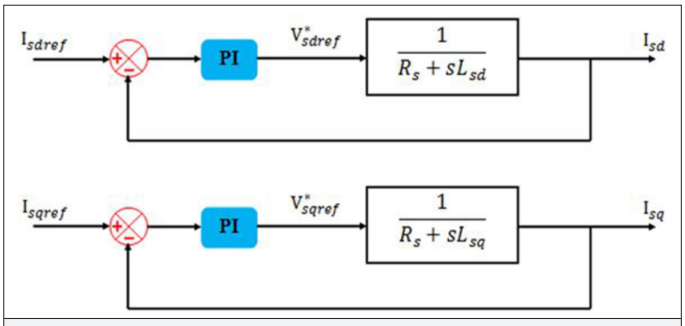

Fig. 3. The current loop diagram after decoupling.

The motor speed control is composed of two nested loops: an inner current loop with a fast response and an outer relatively slow speed loop presented in Fig. 4. [27].

B. Direct Torque Control

The reference frame linked to the stator makes it possible to estimate the flux, the torque, and the position of the stator flux. The purpose of switch control is to give the vector representing the stator flux the direction determined by the reference value [7, 14-15, 28]. The stator flux is calculated by (4), which gives the two flux components. In the sampled numerical space, it is given by (5).

The DTC control consists of directly controlling the commutations of the arms of the inverter by exploiting the torque and flux calculations from (5) and (6) [9, 14-16, 28].

$$\begin{cases} \varphi_{s\alpha} = \int_0^t \left(V_{s\alpha} - R_s I_{s\alpha}\right) dt \\ \varphi_{s\beta} = \int_0^t \left(V_{s\beta} - R_s I_{s\beta}\right) dt \end{cases} \quad (4)$$

$$\overline{\varphi_s}(k+1) \approx \overline{\varphi_s}(k) + \overline{V_s} T_s \quad \Delta\overline{\varphi_s} \approx \overline{V_s} T_s \quad (5)$$

$$T_{em} = k\left(\overline{\varphi_s} \times \overline{\varphi_r}\right) = k\left|\overline{\varphi_s}\right|\left|\overline{\varphi_r}\right| \sin\delta \quad (6)$$

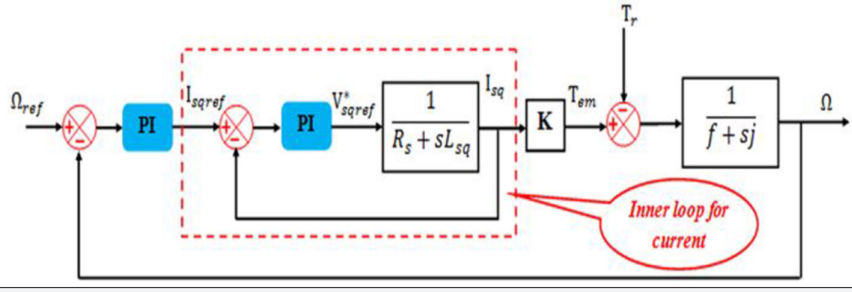

Fig. 4. The inner loop for current and the outer loop for speed.

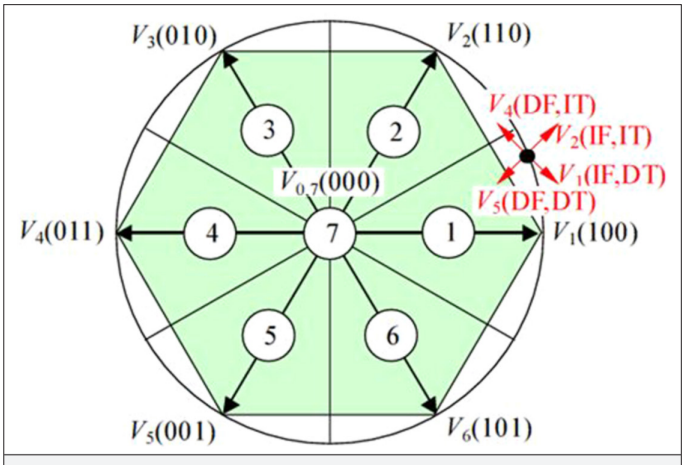

Fig. 5. Control of stator flux and torque with selected stator voltage vectors: 1: on, 0: off, I: increase, D: decrease, F: flux magnitude, T: torque.

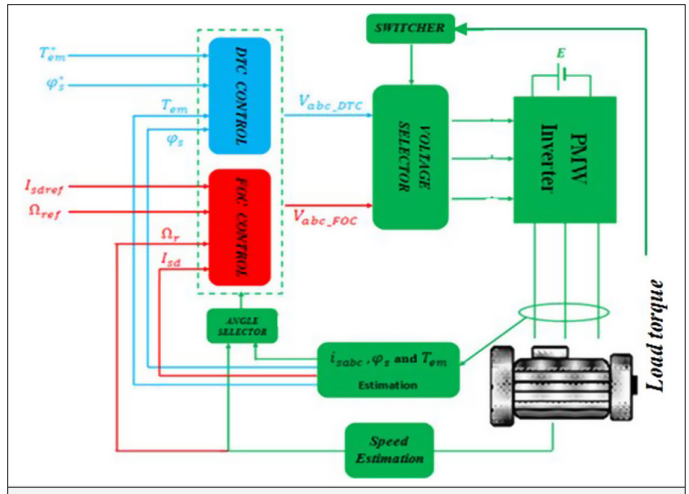

Fig. 6. Principle of proposed control.

Moreover, the stator flux is defined by:

$$\begin{cases} \breve{\varphi}_s = \sqrt{\breve{\varphi}_{s\alpha}^2 + \breve{\varphi}_{s\beta}^2} \\ \angle\breve{\varphi}_s = \tan^{-1}\dfrac{\breve{\varphi}_{s\beta}}{\breve{\varphi}_{s\alpha}} \end{cases} \quad (7)$$

1) Sector Calculation

The states of two hysteresis comparators, one for flux and one for torque, are used to determine the control action taken by the DTC control [28, 29].

Flux is increased by applying a vector pointing in the flux direction, and torque is increased by applying a vector pointing in the rotational direction. So, to choose the appropriate voltage vectors knowledge of the angular position of the stator flux is a primordial action.

Each of the sectors has an angle of 60°. These sectors are numbered as shown in Figure 5, and the angle is calculated by (7). For example 1 represents the sector S_1 for the angle between -30° and 30° [29].

TABLE I. SWITCHING TABLE FOR A CONVENTIONAL DTC

$\Delta\varphi_s$	ΔT_e	S_1	S_2	S_3	S_4	S_5	S_6
1	1	110	010	011	001	101	100
	0	000	000	000	000	000	000
	−1	101	100	110	010	011	001
0	1	010	011	001	101	100	110
	0	000	000	000	000	000	000
	−1	001	101	100	110	010	011

With: $\Delta\varphi_s = \varphi_s^* - \breve{\varphi}_s$; $\Delta T_e = T_{em}^* - \breve{T}_{em}$
φ_s^* : The reference flux; T_{em}^* the reference torque;
$\breve{\varphi}_s$: The estimated flux; $\breve{T}_{em}$: The estimated torque.

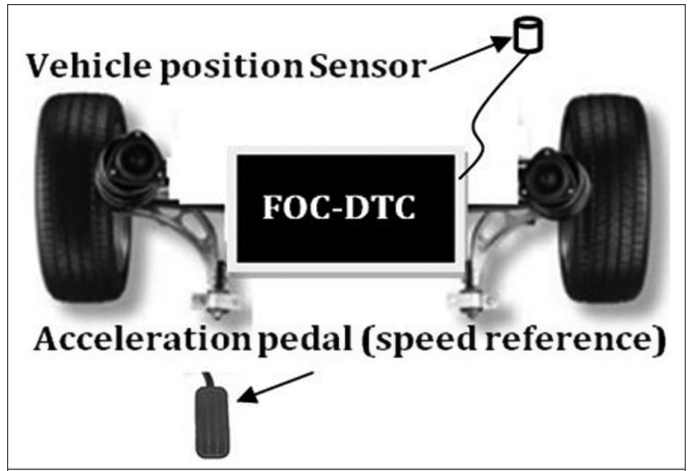

Fig. 7. Location of control devices.

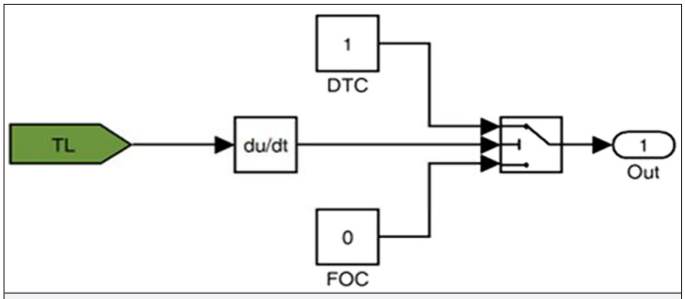

Fig. 8. Switching between the two controls.

TABLE II. PMSM PARAMETERS

Pole pairs	4
Stator resistance (Ω)	1.09
Stator inductance (L_d; L_q)(H)	0.0124
Permanent magnet flux (Wb)	0.1821
Inertia (Kg.m^2)	4.15×10^{-4}

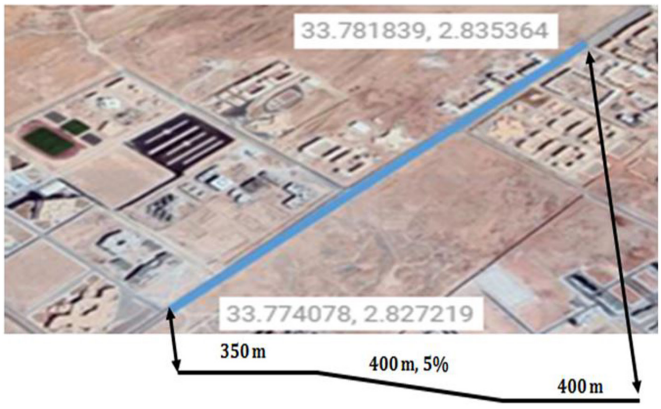

Fig. 9. Picture of experimental path [1].

The switching table used by this control is based on its inputs, which are flux and torque errors and the number of sectors, while its output is the appropriate voltage that must delivered by the inverter. (see Table I).

IV. PROPOSED CONTROL ALGORITHM

We propose to combine the DTC and the FOC to control the PMSM in order to benefit from their advantages (fast control for the torque and fast control for the speed); the principle of this strategy is shown in Fig. 6.

A. Voltage selector (Switcher)

The voltage selector allows selection of the voltage of the DTC or FOC control as appropriate using a switch, which can be activated manually or by obtaining a signal from the position sensor, as indicated in Fig. 7.

When the switch activates one of the controls, the second switches off so as not to consume energy unnecessarily. The vehicle position sensor transmits a signal that allows the instant switching between the two control techniques.

The accelerator pedal is calibrated to determine the speed reference used by the two control techniques, as shown in Fig. 7.

The position of the vehicle implicitly informs us of the necessary torque that must be developed. In addition, we can use the variation of the load torque as a switching set point between the two control techniques (see Fig. 8).

V. STUDY RESULTS

This study uses the same trajectory taken in the work [1] and the PMSM with parameters indicated in Table II.

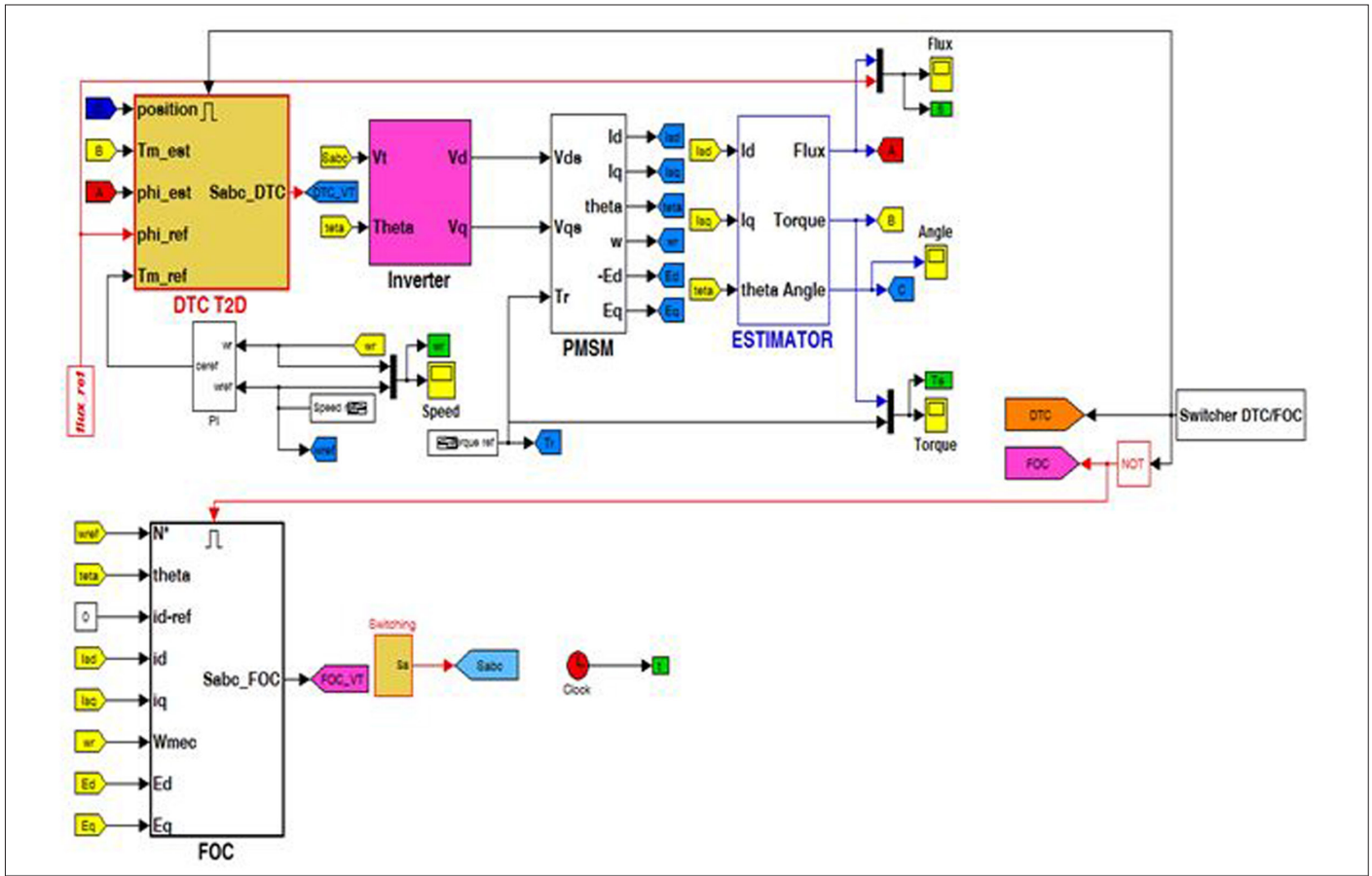

Fig. 10. All blocs of the proposed hybrid control (simulink/matlab©).

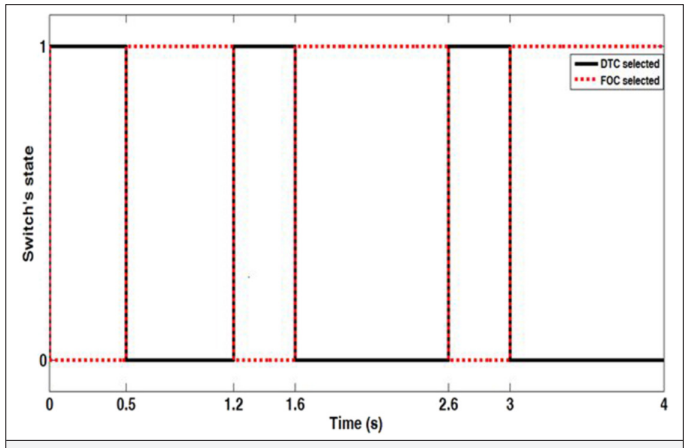

Fig. 11. State of switcher between direct torque control and field-oriented control.

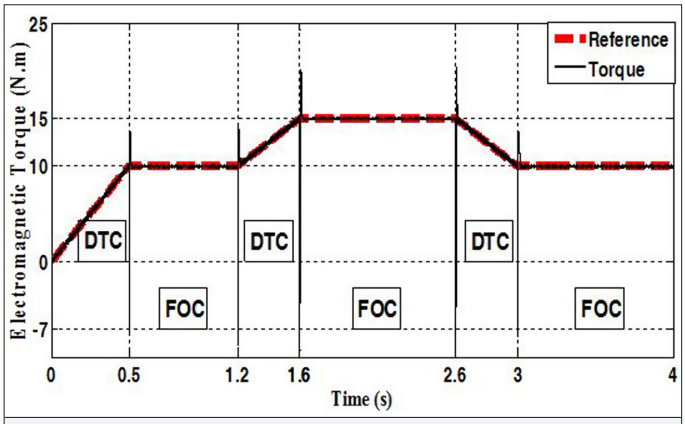

Fig. 12. Electromagnetic and reference torques.

The trajectory is illustrated in Figure 9 it has three phases: the first phase is 400 m without slope, the second phase also has 400 m with a slope of 5%, and the third phase is 350 m without slope.

During the first phase and at start-up, we begin by applying the DTC control; afterward, we switch directly to the FOC control, always keeping the speed at a value of 40 km/h. From the beginning of the second phase, we switch to the DTC control with an increase in speed to 60 km/h. At the beginning of the third phase, we switch to the FOC control with an instantaneous decrease in speed to 40 km/h.

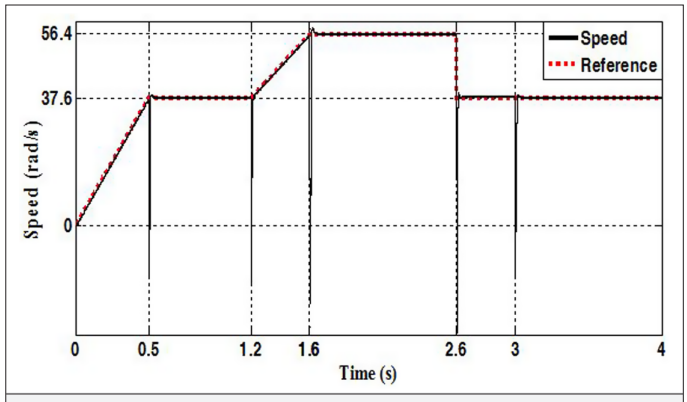

Fig. 13. Estimated speed with its referential.

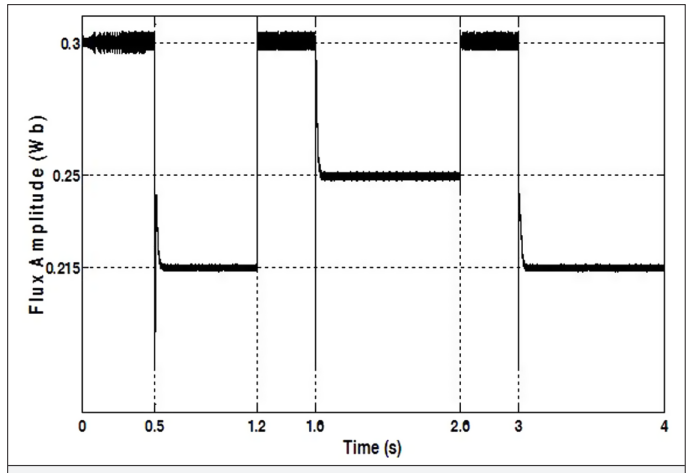

Fig. 14. Amplitude of electromagnetic flux.

By transforming the linear speed to the angular speed, with the use of a car wheel of 59.1 cm (ex / 205/45 R 16), the angular speeds will be 37.60 rad/s, 56.4 rad/s, and 37.6 rad/s successively.

The total simulation time is 91.5 seconds, which is too long a time to simulate the system; for that, we adopt a time scale.

In Fig. 10, we present all parts of the simulation model in the Simulink/Matlab environment.

The results are divided into three parts and illustrated in the figures below.

A. MECHANICAL MAGNITUDES

Figure 11 illustrates the states of the DTC and FOC switcher on the trajectory taken as reference. The switcher is configured in such a way as to change its state when they detect a value greater

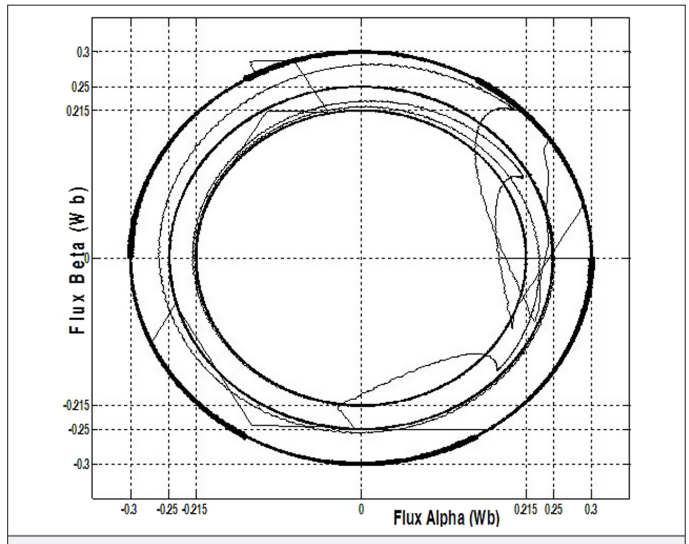

Fig. 15. Electromagnetic flux circle.

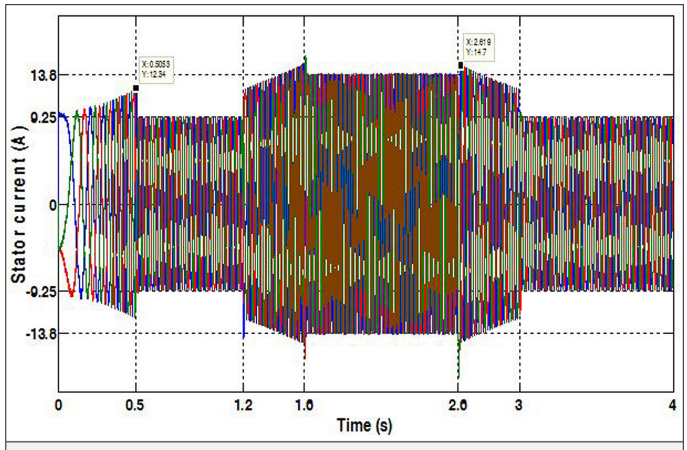

Fig. 16. Stator current.

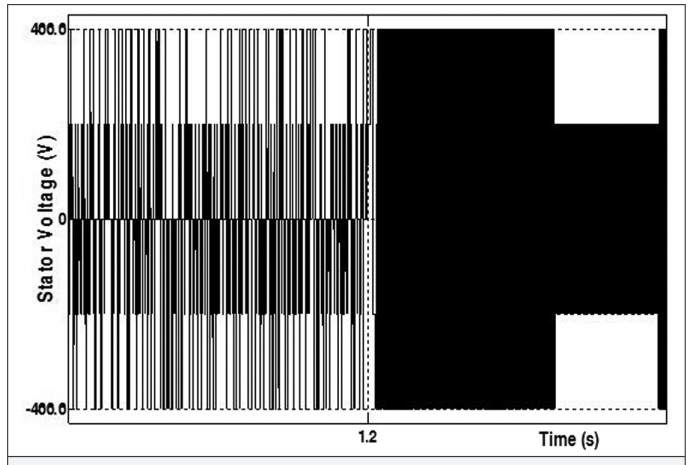

Fig. 18. Stator voltage (Zoom).

than a predefined threshold of the load torque and force the control to switch between the two strategies. In our study, we have set as permutation criterion the derivative of the load torque: when the load is constant the load torque derivative is zero and the switch actuates the FOC and when the load varies the torque derivative becomes non-zero and the switch actuates the DTC as shown in Fig. 8.

Figure 12 shows the shape of the electromagnetic torque with the applied load torque. The electromagnetic torque suitably follows its reference.

At the instant of switching between the two controls, peaks appear but only last for a very short time. The probable cause of these peaks is the initial state of the controlled quantities, which influence the numerical resolution of the system. We estimate that they do not actually occur because of the system's inertia.

Figure 13 shows the shape of the speed following an application of the desired reference speed. We chose at time 2.6 s an abrupt variation of the reference speed to see the robustness of the control in such a case. We can clearly see that the system is well controlled and stable (Table III)

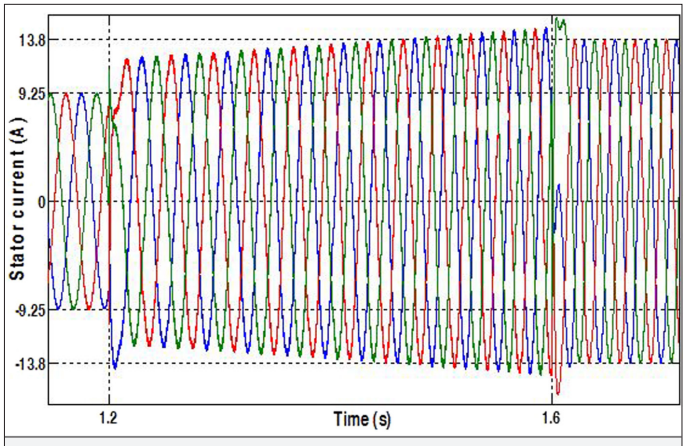

Fig. 17. Stator current (Zoom).

TABLE III. NOMENCLATURE

$V_{s\alpha}$, $V_{s\beta}$	Stator voltages in (α,β) frame
$I_{s\alpha}$, $I_{s\beta}$	Stator currents in (α,β) frame
$\varphi_{s\alpha}$, $\varphi_{s\beta}$	Stator magnetic flux in (α,β) frame
V_{sd}, V_{sq}	Stator voltages in (d,q) frame
I_{sd}, I_{sq}	Stator currents in (d,q) frame
φ_{sd}, φ_{sq}	Stator magnetic flux in (*d, q*) frame
$e_{s\alpha}$, $e_{s\beta}$	Induced electromotive forces in (*d, q*) frame
φ_s	Stator magnetic flux
φ_f	Rotor magnetic flux (permanent magnet)
T_{em}	Electromagnetic torque
T_r	Resistant torque
T_f	Viscous friction torque
Ω	Mechanical speed
P	Number of pole pairs
R_s	Stator resistance
$L_{s\alpha}$, $L_{s\beta}$	Inductances in (α,β) frame
L_{sd}, L_{sq}	Inductances in (d,q) frame
J	Moment of inertia
F	Coefficient of viscous friction
Ω_{ref}	Mechanical reference speed
θ	Position
T_s	Sampling time: 5×10^{-6} s

B. Magnetic Magnitudes

Figures 14 and 15 show the evolution of stator magnetic flux. We note that it is maintained equal to its reference 0.3 Wb during the application of the DTC and drops when the FOC is activated. This boils down to the fact that the DTC controls the flux, and the FOC does not.

C. Electrical Magnitudes

We can see in Figure 16 that the current absorbed during the application of the DTC is stronger than that of the FOC. The FOC is essentially based on control via the current, and in the intervals where this command is applied, the torque is constant, and therefore the current is also constant. On the other hand, the DTC is applied when the torque varies and consequently the absorbed current.

Figure 17 shows the balanced sinusoidal form of the current and its increase when the DTC is selected. This makes the FOC much better than the DTC because for the same driven load it is important to have a low absorbed current.

In Figure 18, we present a zoom of the evolution of the supply voltage of one stator phase. We zoom in on switching times of 1.2 s to highlight the difference between the two voltages delivered by the inverter.

We can see that the inverter switches during DTC take longer in the on position than during FOC, and therefore the inverter is more relieved when the DTC is switched.

VI. CONCLUSION

In this paper, an electric control system that combines the two strategies FOC and DTC has been proposed for the propulsion of an electric vehicle. This proposal aims to exploit the robustness of each technique in the appropriate case. Additionally, we will always have the possibility of using a control block if the other presents a malfunction during the driving of the electric vehicle. An automatic switch sensitive to the variations of the resistive torque, which is a function of the slope of the trajectory of the vehicle, is used to switch between the two control strategies. The results obtained show a good robustness of the driven system and indicate that this combination can ensure the good operation of the propulsion system. It is quite clear that the results obtained are better than those obtained by [2]: the torque, the speed, and the stator flux all have all less ripples.

Our perspective is to improve this control by applying intelligent techniques and implementing them on a DSP or FPGA.

Availability of Data and Materials: The data that support the findings of this study are available on request from the corresponding author.

Peer-review: Externally peer reviewed.

Author Contributions: Concept – S.T., B.M.; Design – S.T., B.M.; Supervision – B.M.; Resources – S.T., B.M.; Materials – S.T., B.M.; Data Collection and/or Processing – S.T., B.M.; Analysis and/or Interpretation – S.T., B.M.; Literature Search – S.T., B.M.; Writing – S.T., B.M.; Critical Review – B.M.

Acknowledgments: We would like to thank Mr. KHALFA Sayeh, a teacher at the English department of the University of Laghouat, for the linguistic revision of this paper.

Declaration of Interests: The authors have no conflict of interest to declare.

Funding: The authors declared that this study has received no financial support.

REFERENCES

1. M. Linani, B. Mokhtari, A. Cheknane, and H. S. Hilal, "Experimental study of a novel filter structure designed for MEMS-based sensors in electric vehicles," *IET Power Electron.*, vol. 12, no. 15, pp. 4063–4069, 2019. [CrossRef]
2. L. Wang, K. Xiao, L. de Lillo, L. Empringham, and P. Wheeler, "PI controller relay auto-tuning using delay and phase margin in PMSM drives," *Chin. J. Aeronaut.*, vol. 27, no. 6, pp. 1527–1537, 2014. [CrossRef]
3. O. A. Omar, "Direct Torque Control of the Permanent Magnet Synchronous Machine Using Intelligent Techniques (Fuzzy Logic, Neural Networks, Genetic Algorithm and PSO), (Commande directe du couple de la machine synchrone à aimants permanents par l'utilisation des techniques intelligentes (logique floue, réseaux de neurones, algorithme génétique et PSO)", Doctoral dissertation. Algeria: Sidi Belabbes University, 2021.
4. I. Omrane, *Development of Software Position Sensors for the Control of the Permanent Magnet Synchronous Machine*, (*Développement de Capteurs Logiciels de Position pour la Commande de la Machine Synchrone à Aimants Permanents*), Doctoral dissertation. France: Poitiers University, 2014.
5. L. J. Cheng, and M. C. Tsai, "Enhanced model predictive direct torque control applied to IPM motor with online parameter adaptation," In *IEEE Access*, vol. 8, pp. 42185–42199, 2020. [CrossRef]
6. Y. Wen, H. Zheng, F. Y. X. Zeng, and X. Zeng, "A novel MTPA and flux weakening method of stator flux oriented control of PMSM," *Transp. Saf. Environ.*, vol. 3, no. 3, 2021. [CrossRef]
7. A. Ameur, B. Mokhtari, N. Essounbouli, and F. Nollet, "Modified Direct Torque Control for Permanent Magnet Synchronous Motor Drive Based on Fuzzy Logic Torque Ripple Reduction and Stator Resistance Estimator", *CEAI*, vol. 15, no. 3, 2013, pp. 45–52. [CrossRef]
8. M. L. Sepulchre "For optimizing the control of permanent magnet synchronous machines at high speed for electric vehicles, (Pour l'optimisation de la commande des machines synchrones à aimants permanents en régime de haute vitesse pour véhicule électrique)". Doctoral dissertation. France: Toulouse University, 2017.
9. B. Chourouk, *Modeling, Control and Diagnosis of Synchronous Magnet Machines*, (*Modélisation, Commande & Diagnostic des Machines Synchrones à Aimants*). Doctoral dissertation. Algeria, 2018, p. 2.
10. H. Jiacai, L. Hongsheng, X. Qinghong, and L. Di, "Sensorless vector control of PMSM using sliding mode observer and fractional-order phase-locked loop," in *Proceedings of the 31st Chinese Control Conference*, 2012, pp. 4513–4518.
11. A. Ngon, "Comparative study of the power chain of electric vehicles.", ("Etude comparative de la chaine de puissance des véhicules électriques"), Thesis, 2020. Canada: Québec à Trois Rivières University. Available: https://depot-e.uqtr.ca/id/eprint/9290.
12. A. Dutt, A. Gauri, and V. B. R, "Sensorless direct torque control techniques for induction motor drives: A status review," International Conference on Control., Communication and Computing (ICCC), Thiruvananthapuram, India, vol. 2023, 2023, pp. 1–6. [CrossRef]
13. G. Faten, and S. Lassaâd, "Speed sensorless IFOC of PMSM based on adaptive Luenberger observer," *Int. J. Comput. Electr. Autom. Control. Inf. Eng.*, vol. 4, no. 8, 2010.
14. A. Ameur, B. Mokhtari, L. Mokrani, N. Essounbouli, and B. Azoui, "Extended Kalman Filter for Speed Sensorless Direct Torque control of a Permanent Magnet Synchronous Motor Drive Based Stator Resistance Estimator," *J. Electr. Control. Eng.*, vol. 2, no. 6, pp. 33–39, 2012.
15. A. Ameur, B. Mokhtari, N. Essounbouli, and L. Mokrani, "Speed sensorless direct torque control of a PMSM drive using space vector modulation based MRAS and stator resistance estimator," *World Acad. Sci. Eng. Technol.* vol. 6, 2012.
16. A. Aissa, K. Ameur, and B. Mokhtari, "MRAS for Speed sensorless direct torque control of a PMSM drive based on PI fuzzy logic and stator resistance estimator," *Trans. Control. Mech. Syst.*, vol. 2, no. 7, pp. 321–326, 2013.
17. A. Aissa, *Speed Sensorless Control by DTC of a Synchronous Machine with Permanent Magnets Equipped with a Complete Order Observer with Sliding Modes*, (*Commande sans Capteur de Vitesse par DTC d'une Machine Synchrone à Aimants Permanents Dotée d'un Observateur d'Ordre Complet à Modes Glissants*), Doctoral dissertation. Algeria, 2012, p. 2.
18. S. Pradhan, A. K. Sahoo, and R. K. Jena, "Comparison of DTC and SVM - DTC of Induction motor drive for Electric Vehicle application," International Conference on Intelligent Controller and Computing for Smart Power (ICICCSP), Hyderabad, India, vol. 2022, 2022, pp. 1–6. [CrossRef]
19. M. El Mahfoud, B. Bossoufi, N. El Ouanjli, S. Mahfoud, and M. Taoussi, "Three Speed controllers of direct torque control for a doubly fed

induction motor drive–A comparison," *Electrica*, vol. 21, no. 1, pp. 129–141, 2021. [CrossRef]
20. S. Guedida, B. Tabbache, K. Nounou, and A. Idir, "Reduced-Order Fractionalized Controller for Disturbance Compensation Based on Direct Torque Control of DSIM With Less Harmonic", *ELECTRICA*, vol. 24, no. 2, pp. 450–462, 2024. [CrossRef]
21. U. Kitis, and Y. Üser, "Determination and control of the instant moment need of electric vehicles in variable road conditions with a Lyapunov-based flux observer," *Electrica*, vol. 21, no. 3, pp. 428–443, 2021. [CrossRef]
22. C. Habib, "Contribution to the Integration of a FACTS Interface for a Wind Farm Based on Permanent Magnet Synchronous Machines, (Contribution à l'Intégration d'une Interface FACTS pour une Ferme Éolienne Basée sur des Machines Synchrones à Aimant Permanent)"; *Doctoral dissertation*. Algeria: Sidi Belabbes University, 2018.
23. N. Maleki, and M. R. A. zadeh Pahlavani, "A detailed comparison between FOC and DTC methods of a permanent magnet synchronous motor drive," *J. Electr. Electron. Eng.*, vol.3, no. 2, pp. 92–100, 2015. [CrossRef]
24. M. S. Merzoug, and F. Naceri, "Comparison of field-oriented control and direct torque control for permanent magnet synchronous motor (PMSM)," *World Acad. Sci. Eng. Technol. Int. J. Electr. Comput. Electron. Commun. Eng.*, vol. 2, no. 9, 2008.
25. G. F. Abdelnaby, T. A. Dakrory, S. H. Arafa, and S. G. Ramdan, "Sensorless field oriented control of permanent magnet synchronous motor," *Int. J. Curr. Eng. Technol.*, vol. 5, no. 1, 2015.
26. S. G. Malla, and J. M. R. Malla, "Sensorless control of permanent magnet synchronous motor (PMSM)," *Int. J. New Technol. Sci. Eng.*, vol. 1, no. 2, 2014.
27. A. ElShahat, and H. ElShewy, "PM synchronous motor drive system for automotive applications," *J. Electr. Syst.*, vols. 6–2, 2010.
28. K. Chikh, A. Saad, M. Khafallah, D. Yousfi, F. Z. Tahiri, and M. Hasoun, "A constant switching frequency DTC for PMSM using low switching losses SVM-an experimental result," *IJPEDS*, vol. 8, no. 2, pp. 558–583, 2017. [CrossRef]
29. B. Mokhtari, and M. F. Benkhoris, "High ripples reduction in DTC of induction motor by using a new reduced switching table," *J. Electr. Eng.*, vol. 67, no. 3, pp. 206–211, 2016. [CrossRef]

Saad TAA was born in Tiaret, Algeria, in 1983. He received the Engineer degree in Electromechanics from the Electrical Engineering Department of Tiaret University in 2007, and then he received the Magister in Industrial Control of Electrical Drives and Diagnostics from the Electrical Engineering Department of Oran University in 2013. His research interest is Electrical Machine Control.

Bachir MOKHTARI was born in Laghouat, Algeria, in 1971. He received the Engineer degree in Electrical Machines from the Electrical Engineering Department of Laghouat University in 1997, and then he received the Magister and the DSc degrees in Electrical Engineering from the Electrical Engineering Department of Batna University in 2004 and 2014, respectively. Since 2014, he is an Associate Professor in the Electrotechnics Department of Laghouat University. His research interests include Electrical Machines Control and Renewable Energies and their applications.